

# THE STABILITY OF GRANULAR AND COHESIVE MATERIALS IN TRIAXIAL COMPRESSION

By Norman W. McLeod, Engineering Consultant  
Department of Transport, Ottawa, Canada

## Introduction

The fundamental principles developed in this paper are applicable to soil mechanics in general, but their use is illustrated here with regard to the selection of base course materials and to the design of bituminous paving mixtures.

Fig. 1 provides a diagram of possible planes of shearing failure under a loaded area on the surface of an airport or highway. It is the principal problem of design to avoid detrimental shear in the subgrade, base course, and wearing surface. If sufficient plastic shear develops in any one or more of these three elements, rutting and upheaval of the surface will occur.

Detrimental plastic shear of the subgrade is prevented by an adequate overlying thickness of base course and

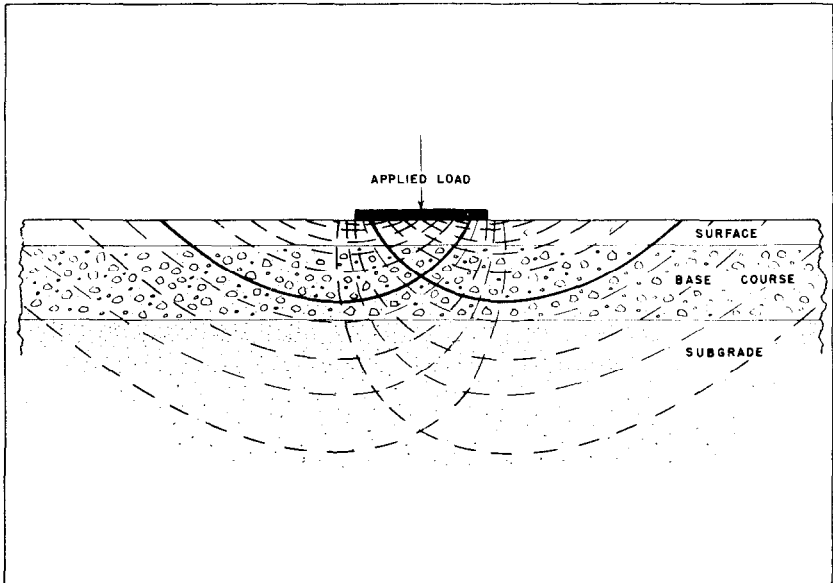


Fig. 1. Diagram of Shear Planes under a Loaded Area

pavement.<sup>1,2</sup> However, the base course material and the flexible surface must also each possess the required stability (resistance to plastic shear) under the imposed stress.

It is a serious drawback to the design of bituminous pavements and granular base courses at the present time, that it cannot be placed on the basis of pounds per square inch, in terms of flexural strength, shear, or similar property, as is the case for the design of steel columns or girders, rigid pavements, etc. In addition, there is the difficult problem of finding a common basis for comparing the stabilities of the various base course materials available for any project, and the stabilities of bituminous mixtures made from the different aggregate materials at hand, in order that the most economical selection of each may be made.

The development which follows, indicates that the triaxial compression test can provide a fundamentally sound basis of comparison for the selection of base course and aggregate materials insofar as their stability is concerned, and that it can be utilized for designing the stability or strength of flexible bases and wearing surfaces on a p.s.i. basis.

A triaxial compression test differs from an ordinary compression test, in that provision is made for controlled lateral support while the specimen is subjected to vertical load. Fig. 2 is a diagram of the essential equipment for this test. To the lucite cylinder, the two metal end pieces are fitted by means of water-tight and air-tight gasketed joints. A cylindrical specimen of the material to be tested is inserted in a rubber sleeve between porous stones at top and bottom. By means of connections through the porous stones, the material within the rubber sleeve can be subjected to either vacuum or water pressure, if desired. Water or air can be pumped into the lucite cylinder to provide the magnitude of lateral support required when testing each specimen. The rubber sleeve prevents water within the lucite cylinder from entering the sample. Each specimen is subjected to a constant lateral pressure throughout the test, and increasing vertical load is applied in a standard manner until it fails. A complete triaxial compression test usually consists of loading three or four cylindrical specimens of a given material to failure, employing a different degree of lateral support for each specimen, eg., 0, 15, 30 and 60, p.s.i.

The data obtained from testing a given material in triaxial compression are plotted in the form of a Mohr diagram, fig. 3. The applied lateral pressure  $L$ , and the

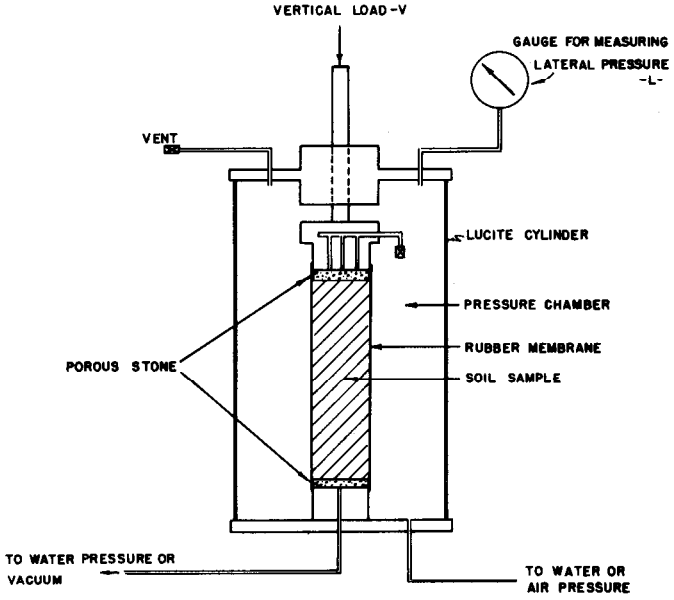


Fig. 2. Sketch of Apparatus for Triaxial Compression Test

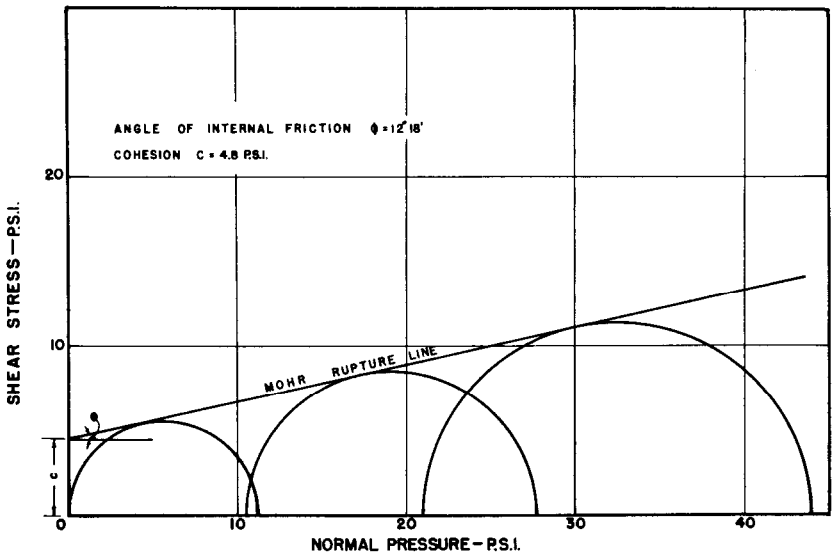


Fig. 3. Typical Mohr Diagram for Triaxial Compression Test

corresponding vertical pressure  $V$  which caused failure, are marked off on the horizontal axis for each test specimen. Using the difference between the vertical and lateral pressure,  $V - L$ , for each specimen as the diameter, semi-circles, known as Mohr circles, are described. The tangent which is common to the Mohr circles is drawn and produced to intersect the vertical axis. The intercept made on the vertical axis is designated cohesion  $c$ , from the Coulomb equations  $s = c + n \tan \phi$ , while the angle between the common tangent and the horizontal is the angle of internal friction  $\phi$ .

The common tangent is generally known as the Mohr rupture line or Mohr envelope. All semi-circles which are tangent to or below the Mohr envelope, represent equilibrium or stable relationships respectively, between corresponding values of lateral pressure  $L$  and vertical pressure  $V$ . Any semi-circle which cuts through the Mohr envelope, indicates corresponding combinations of lateral pressure  $L$  and vertical pressure  $V$  which would cause failure of the material being tested.

For the development which follows, it is assumed that the Mohr envelope is a straight line. This assumption appears to be justified on the basis of recent published reports by Holtz<sup>3</sup>, Rutledge<sup>4</sup>, and Nijboer,<sup>5</sup> and others.

The Mohr diagram provides a fundamental basis for defining the term "stability" as applied to granular and cohesive materials in general, and to flexible base course and surfacing materials in particular. Granular and cohesive materials may be classified in terms of increasing stability according to their capacity for carrying a greater applied vertical load  $V$  for a given value of lateral support  $L$ . Consequently, for the equilibrium conditions of stress established by the Mohr envelopes for a number of materials under comparison, for any specified value of lateral support  $L$  the most stable material is that for which the value  $(V - L)$  is greatest.

While the terms, vertical load  $V$ , and lateral support  $L$ , as they are frequently designated for the triaxial test, will be employed throughout this paper, it is to be understood that they have the significance, in the widest sense, of major and minor principal stresses respectively, which are usually denoted by  $\sigma_1$  and  $\sigma_3$ .

By reference to the Mohr diagram, cohesive and granular materials can be conventionally divided into three groups:

- (a) purely cohesive materials, i.e., those having a positive value for cohesion  $c$ , but for which the angle of internal friction  $\phi$  is zero, fig. 4.

Saturated clays in the quick triaxial test approximate these requirements.

- (b) purely granular materials, i.e., those having a positive value for the angle of internal friction  $\phi$ , but for which the cohesion  $c$  is zero, fig. 6. Clean sands and gravels approach this condition.
- (c) materials which have both granular and cohesive properties, i.e., those having positive values for both  $c$  and  $\phi$ , fig. 3. Bituminous paving mixtures, mechanically stabilized base courses with positive values for plasticity index, and remolded clays, are common examples.

## 2. The Stability of Purely Cohesive Materials

Fig. 4 illustrates the Mohr diagram for a purely cohesive material. The angle of internal friction  $\phi$  is zero. The Mohr envelope is parallel to the abscissa, and at a distance  $c$  from it. Regardless of the magnitude of the lateral support  $L$ , the diameter of any Mohr circle, that is of  $(V - L)$ , which represents the stability of the material, is a constant for any specified value of  $c$ .

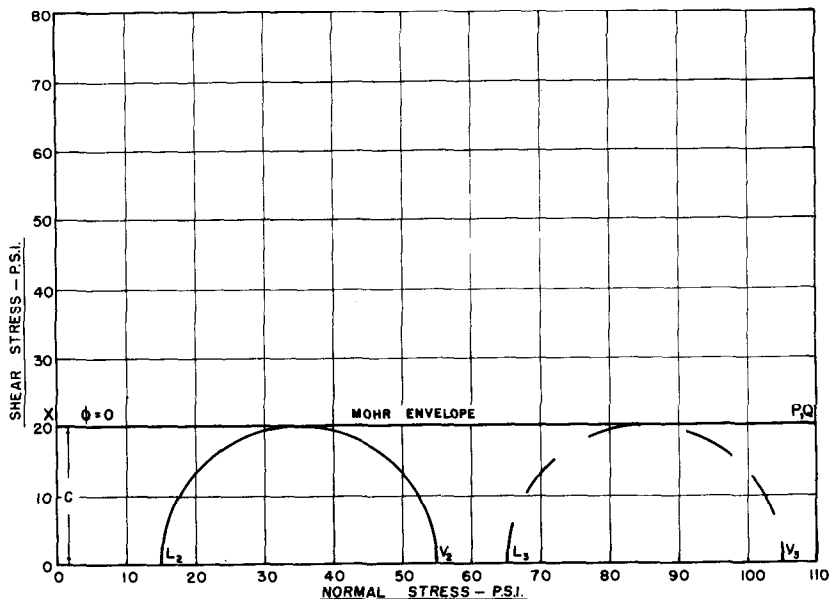


Fig. 4. Mohr Diagram for Materials Having Zero Angle of Internal Friction in Triaxial Compression

The mathematical equation of stability for a purely cohesive material is, therefore.

$$V - L = 2c \tag{1}$$

and the stability diagram for a purely cohesive material, based upon this equation, is shown in fig. 5.

If a vertical load  $V$  of 150 p.s.i. were to be supported by a base course which could develop a maximum lateral support  $L$  of 50 p.s.i., equation (1) and fig. 5 indicate that a purely cohesive material with cohesion  $c$  equal to 50 p.s.i., minimum, would be required to provide the necessary stability.

### 3. The Stability of Purely Granular Material

From fig. 6, a Mohr diagram for purely granular materials, it is apparent that the stability value ( $V - L$ ) depends upon the magnitude of the lateral support  $L$ , and the size of the angle of internal friction  $\phi$ .

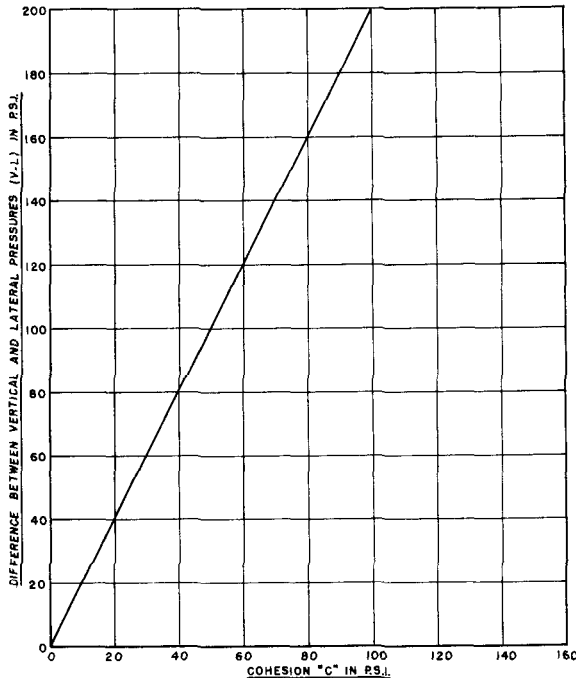


Fig. 5. Stability Diagram in Terms of (V-L) and Cohesion "C" for Materials Having Zero Angle of Internal Friction in Triaxial Compression

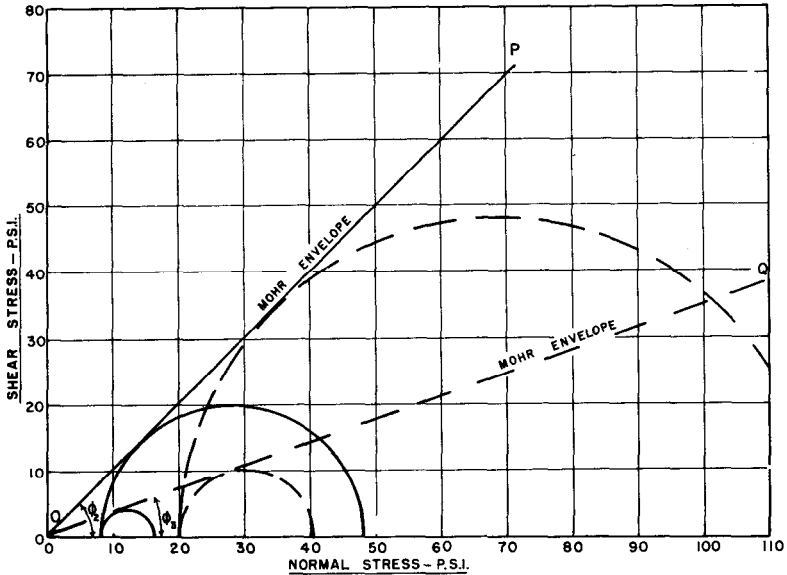


Fig. 6. Mohr Diagram for Materials Having Zero Cohesion in Triaxial Compression

From a study of the trigonometrical relationships of fig. 7, it follows that,

$$r = \frac{L \sin \phi}{1 - \sin \phi} \quad (2)$$

and

$$V - L = 2r \quad (3)$$

Therefore,

$$V - L = \frac{2L \sin \phi}{1 - \sin \phi} \quad (4)$$

Equation (4) is a mathematical equation for the stability,  $(V - L)$ , of purely granular materials. When equation (4) is plotted in terms of  $(V - L)$  curves for different values of lateral support  $L$ , and of angle of internal friction  $\phi$ , the stability diagram of fig. 8 is obtained.

If a base course is to carry a vertical load  $V$  of 150 p.s.i., and can develop a maximum lateral support  $L$  of 50 p.s.i., then its stability requirement,  $(V - L)$ , is 100 p.s.i. Either equation (4) or fig. 8 indicates that a purely granular material with an angle of internal friction  $\phi = 30^\circ$  or greater, would be required to provide the necessary stability for this base course.

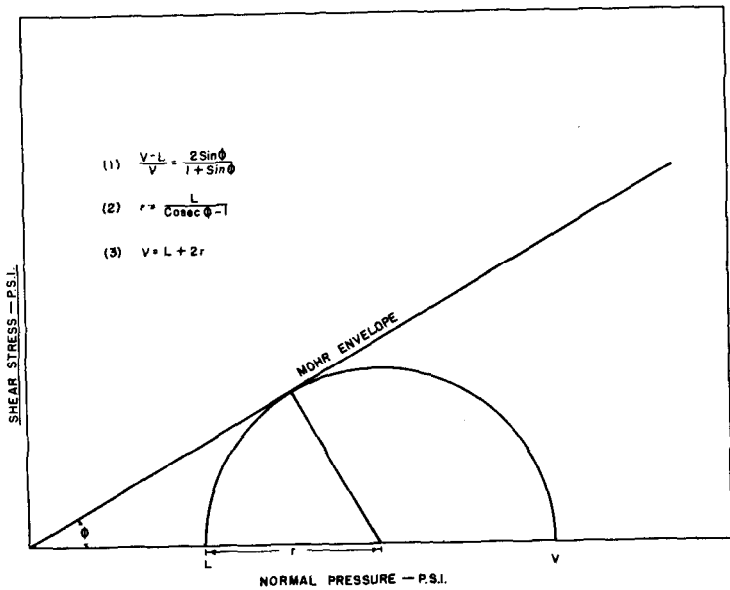


Fig. 7. Trigonometrical Relationship for Mohr Diagram for Materials with Zero Cohesion

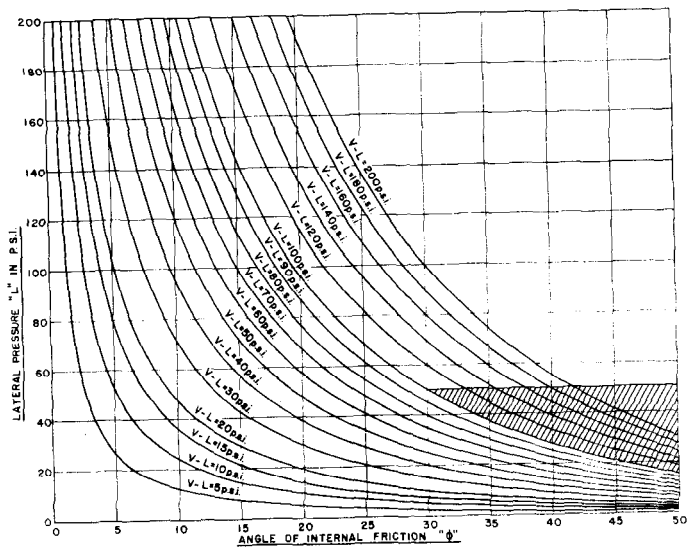


Fig. 8. Stability Diagram in Terms of L,  $\phi$  and (V-L) for Materials Having Zero Cohesion in Triaxial Compression



4. The Stability of Materials With Combined Granular and Cohesive Properties

From fig. 3, it is clear that the stability,  $(V - L)$ , of materials with both granular and cohesive properties, depends upon the magnitude of the lateral support  $L$ , the cohesion  $c$ , and the angle of internal friction  $\phi$ . The geometrical and trigonometrical relationships required for the development of the equation of stability for these materials, are illustrated in fig. 9.

It follows from fig. 9, that,

$$\tan \phi = \frac{\frac{V - L}{2} \cos \phi - c}{L + \frac{V - L}{2} - \frac{V - L}{2} \sin \phi} \tag{5}$$

which can be worked through to

$$V - L = \frac{2 L \sin \phi}{1 - \sin \phi} + 2 c \sqrt{\frac{1 + \sin \phi}{1 - \sin \phi}} \tag{6}$$

The stability diagram of fig. 10 is obtained when equation (6) is plotted in terms of given values of stability

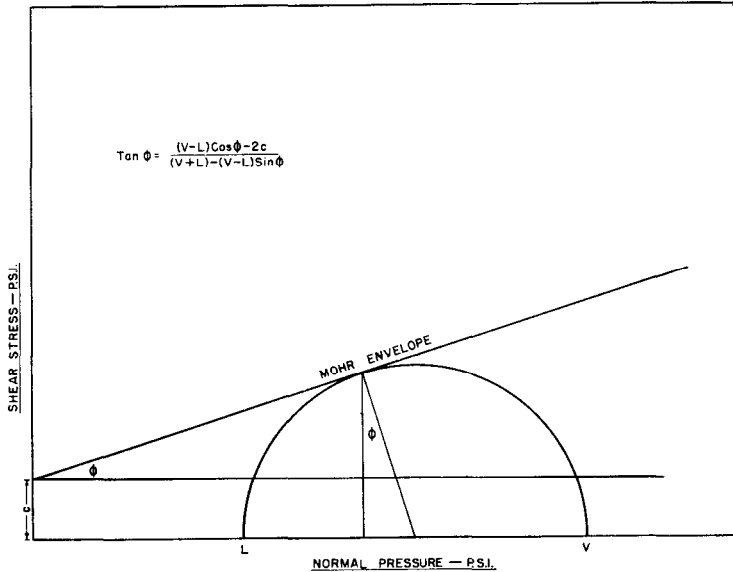


Fig. 9. Trigonometrical Relationships for Mohr Diagram for Materials Having Positive Values of  $C$  and  $\phi$  in Triaxial Compression

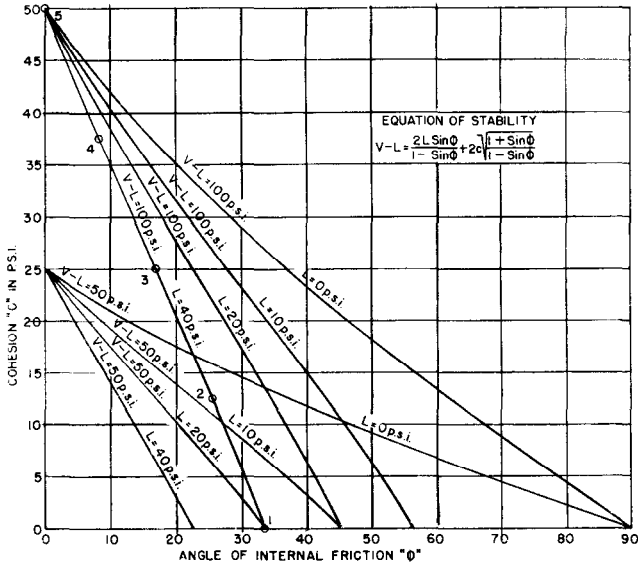


Fig. 10. Stability Diagram in Terms of C, φ, L and (V-L) for Materials Having Positive Values for C and φ in Triaxial Compression

(V - L) for different degrees of lateral support L, and for various magnitudes of c and φ. The (V - L) stability curves of this diagram are not straight lines, although for the intermediate and higher values of lateral support L they are very nearly so. For a lateral support L = 0, the stability curves are concave upwards throughout, while for L equal to any value greater than zero, they are reverse curves.

The stability diagram of fig. 10 may be more readily understood with reference to the Mohr diagram of fig. 11, which contains several Mohr circles of the same diameter, that is, same (V - L) value, but with different degrees of lateral support L. To one of these, (V - L) = 100 p.s.i., and L = 40 p.s.i., several Mohr envelopes have been drawn for some of the infinite combinations of c and φ, that are possible for this particular Mohr circle. The combinations of c and φ corresponding to each of these Mohr envelopes, are shown as points 1, 2, 3, 4, and 5 on the curved line graph of fig. 10, representing (V - L) = 100 p.s.i., and L = 40 p.s.i. That is, points 1, 2, 3, 4, and 5, represent Mohr envelopes AT, BT, CT, DT, and ET of fig. 11, where T is at the point of tangency for each Mohr envelope drawn to the Mohr circle in question.

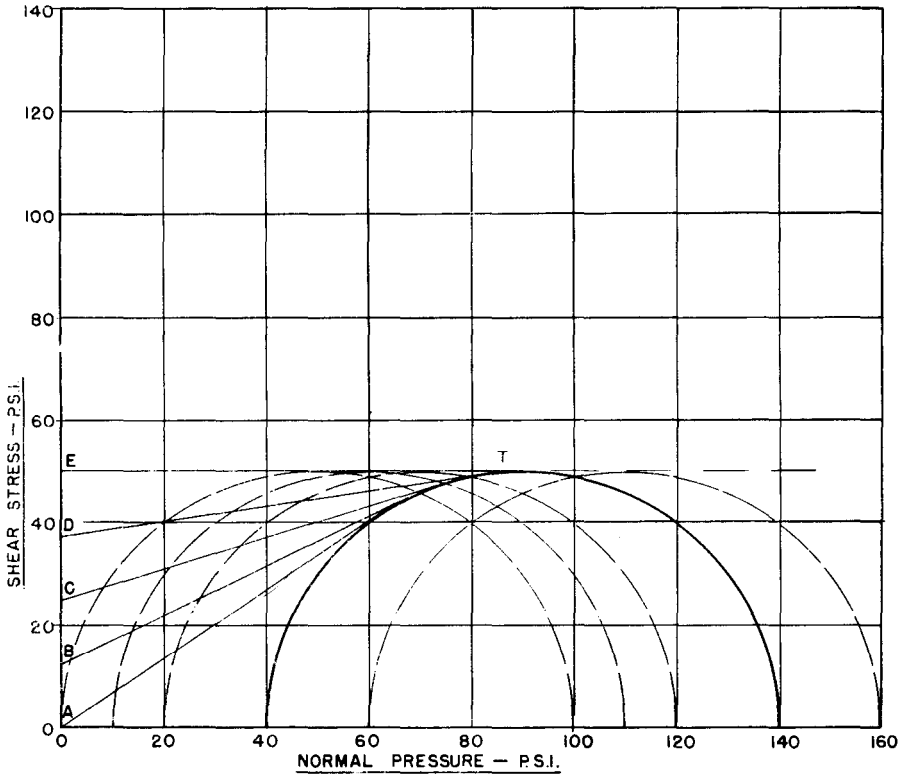


Fig. 11. Mohr Diagram for Constant (V-L) but Varying Lateral Support L

For the curved line representing any one of the infinite combinations of (V - L) and L values that are possible in fig. 10, there are very simple equations for locating the extremities of the line on the c and  $\phi$  axis.

When  $\phi = 0$ , equation (6) reduces to equation (1)

$$V - L = 2c \quad (1)$$

and this locates the required extremity of the line on the c axis.

When  $c = 0$ , the extremity of this line on the  $\phi$  axis can be obtained from the equation

$$\sin \phi = \frac{V - L}{V + L} \quad (7)$$

Referring again to the problem of designing a base course to carry a vertical load  $V$  of 150 p.s.i., and for which the maximum lateral support  $L$  that can be developed is 50 p.s.i., the solution can be calculated by means of equation (6), and is given graphically in fig. 12, which indicates that an infinite number of answers are possible. All materials possessing those combinations of  $c$  and  $\phi$  which are on or to the right of the curve labelled  $(V - L) = 100$  p.s.i.,  $L = 50$  p.s.i., in fig 12, would have the required stability. Materials with those combinations of  $C$  and  $\phi$  which lie within the cross-hatched area to the left of this line would tend to be unstable and therefore unsatisfactory, insofar as this particular base course design problem is concerned.

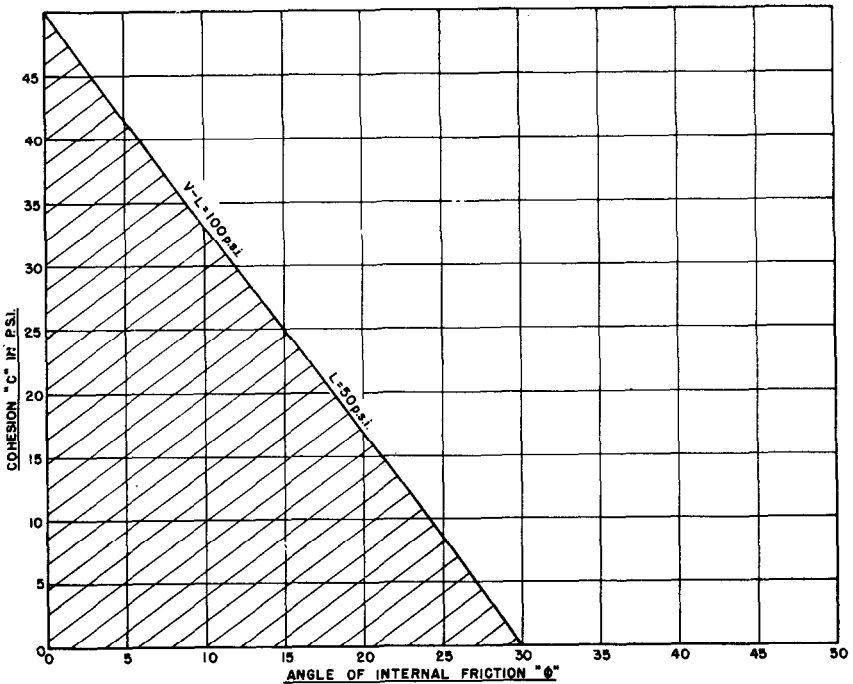


Fig. 12. Stability Diagram in Terms of  $C, \phi, L$  and  $(V-L)$  For Materials Having Positive Values for  $C$  and  $\phi$  In Triaxial Compression

As deposits of good granular material for base courses become depleted, highway and airport engineers are being forced more and more to contemplate the utilization of what have been considered inferior materials. The primary requirement of a base course material is adequate stability under load. By testing inferior gravels, sands, or other materials in triaxial compression, and plotting the location of their corresponding  $c$  and  $\phi$  values on a stability diagram like that of fig. 10, their deficiencies become immediately apparent. The problem with regard to any given inferior material is then largely one of economics, as to whether its  $\phi$  value should be improved by incorporating a good granular material, or its  $c$  value improved by adding suitable binder such as clay, bitumen, portland cement, etc., or whether both a binder and granular material are to be incorporated. If the deficient material can be improved to the extent that under the worst conditions expected for it in the field, its combination of  $\phi$  and  $c$  values will be located to the right of the required ( $V - L$ ) stability curve for the maximum lateral support  $L$  developed by the base course on that project, e.g., fig. 12, it will function as satisfactorily as the most carefully selected aggregate, insofar as base course stability is concerned.

It might be added that this application of the triaxial test would place the design of soil-bituminous mixtures on a sound fundamental basis. Soil bituminous mixtures possess both cohesion and internal friction. By means of the development just outlined, the stabilities of soil-bituminous mixtures could be determined and compared directly with those for granular base course materials on a pounds per square inch basis.

##### 5. The Design of Bituminous Mixtures

Regardless of the magnitude of their stability as determined by the triaxial compression test, it is common knowledge that gravel road surfaces which contain no binder of any kind, develop washboard and other indications of instability under the particular types of stresses to which the surface layer is subjected by motor vehicle and aeroplane traffic. Experience has shown that for satisfactory performance, the surface layer of a highway or airport must contain a binding material to give it cohesion. The most commonly employed binders are clay, bitumen and Portland cement, and should probably include moisture.

Equation (6) and the stability diagram of fig. 10 are not entirely satisfactory for the design of the surfacing for a highway or airport, since they would permit the

use of materials with even zero cohesion. The problem therefore, is to establish the minimum value of the cohesion  $c$  which is required for surfacing materials, such as bituminous mixtures, and mechanically stabilized mixtures of aggregates and soil binders.

The required minimum value of  $c$  might be determined empirically. It happens however, that there is an approach to this problem, based upon the properties of the Mohr diagram, which provides minimum values for cohesion  $c$  that are in reasonable agreement with the results of experimental studies contained in a diagram in a recent publication of the Asphalt Institute.

The geometrical and trigonometrical relationships required for this approach to the problem are illustrated in fig. 13.

When  $\log \frac{V-L}{V}$  is plotted versus  $\log L$  for the Mohr envelope for any material possessing both cohesive and granular properties, the reverse curve graph of fig. 14 is obtained. The value of the lateral pressure  $L$  at which the point of inflection in fig. 14 occurs, is obtained by

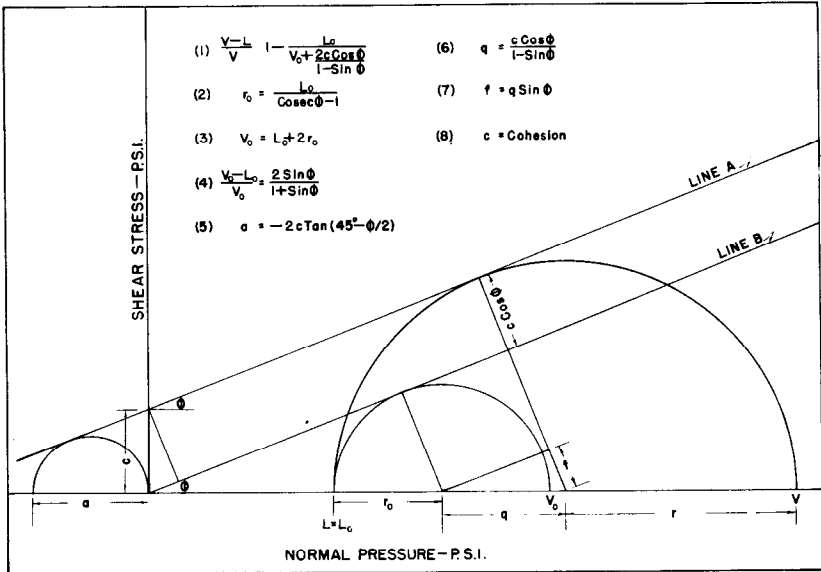


Fig. 13. Diagram Illustrating Certain Geometrical Relationships for Triaxial Compression Test Data

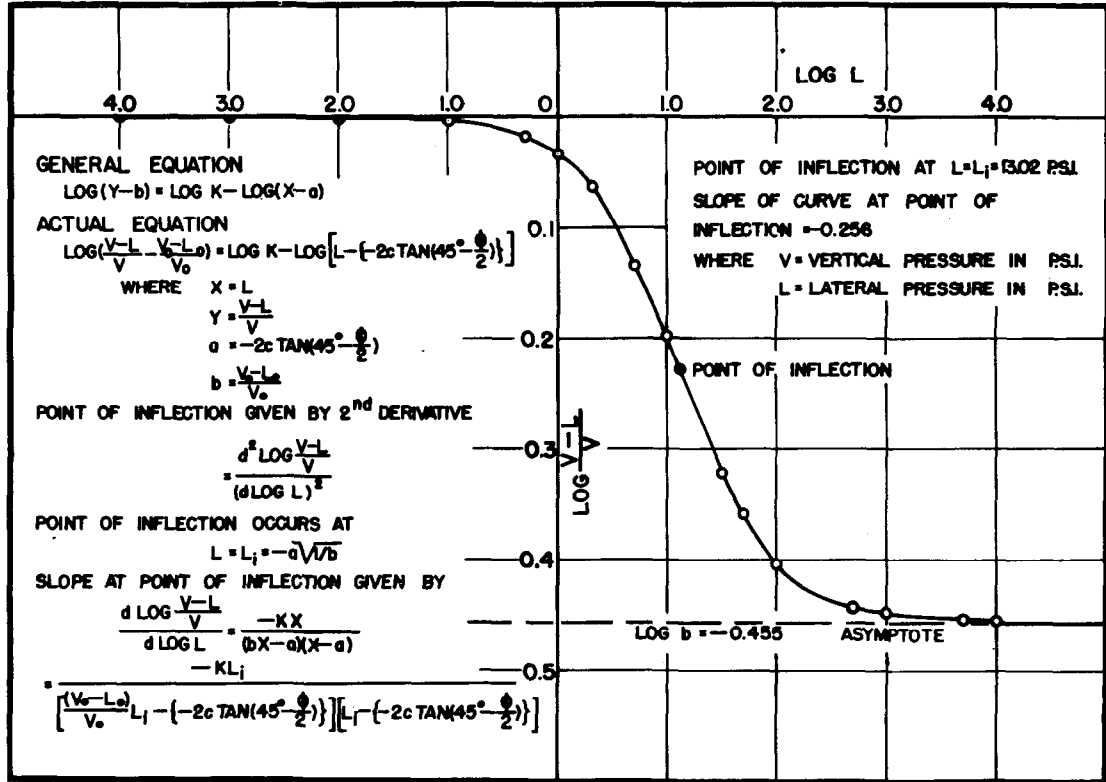


Fig. 14. Log of Ratio  $\frac{V-L}{V}$  Versus Log L for Triaxial Compression Test

equating the second derivative of the equation for the curve to zero. It should be noted that a reverse curve is also obtained when either  $\frac{V - L}{V}$  or  $\frac{L}{V}$  is plotted versus  $\log L$ .

The equations and mathematical derivations involved in obtaining expressions for the value of the slope of this reverse curve at any point, and of the lateral pressure  $L$  at the point of inflection, are outlined in fig. 14.

The term " $L_1$ " is applied to the particular value of the lateral pressure  $L$  at the point of inflection of the curve in fig. 14, and the corresponding vertical pressure  $V$  is represented by " $V_1$ ". For each Mohr envelope, fig. 3, there can be only one value of  $L_1$  and one value of  $V_1$ . That is, for any one combination of values of cohesion  $c$  and angle of internal friction  $\phi$ , there can be only one value of  $L_1$  and its corresponding value of  $V_1$ . Consequently, the corresponding values of  $L_1$  and  $V_1$  are a characteristic of each Mohr envelope.

The expressions for  $L_1$ ,  $V_1$ , and  $(V_1 - L_1)$ , when reduced to their simplest forms in terms of  $c$  and  $\phi$  are as follows, -

$$L_1 = 2c \sqrt{\frac{1 - \sin\phi}{2 \sin\phi}} \tag{8}$$

$$V_1 = 2c \left\{ \frac{1 + \sin\phi + \sqrt{2 \sin\phi} \sqrt{1 + \sin\phi}}{\sqrt{2 \sin\phi} \sqrt{1 - \sin\phi}} \right\} \tag{9}$$

$$(V_1 - L_1) = 2c \left\{ \frac{\sqrt{1 + \sin\phi} + \sqrt{2 \sin\phi}}{\sqrt{1 - \sin\phi}} \right\} \tag{10}$$

$$(V_1 - L_1) = L_1 \left\{ \frac{2 \sin\phi + \sqrt{2 \sin\phi} \sqrt{1 + \sin\phi}}{1 - \sin\phi} \right\} \tag{11}$$

In fig. 15, Mohr circles representing corresponding values of  $L_1$  and  $V_1$  have been drawn to the Mohr envelopes for  $c$  equal to unity in each case, but with values of internal friction  $\phi$  varying from  $1^\circ$  to  $50^\circ$ . In fig. 16, Mohr circles in terms of  $L_1$  and  $V_1$  are drawn to the Mohr envelopes for  $\phi = 30^\circ$  in each case, but with values of  $c$  equal to 10, 20, and 30 p.s.i.

Fig. 15 demonstrates that for a constant value of  $c$ , the value of  $(V_1 - L_1)$  increases as  $\phi$  increases, and vice versa. Fig. 16 indicates that for a constant value of  $\phi$ , the value of  $(V_1 - L_1)$  increases as  $c$  increases, and vice versa. It has long been known that for a given lateral pressure  $L$ , the stability or strength of materials  $(V - L)$  increases, as either  $c$  or  $\phi$  or both increase. Consequently,



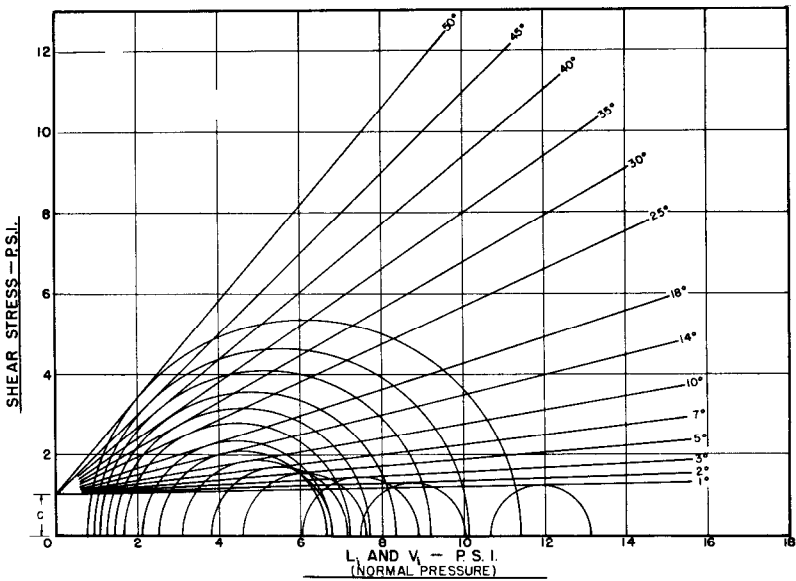


Fig. 15. Mohr Diagram Illustrating Influence of Variation in Angles of Internal Friction " $\phi$ " On Values of  $L_1$  and  $V_1$  When Cohesion " $c$ " Is Constant

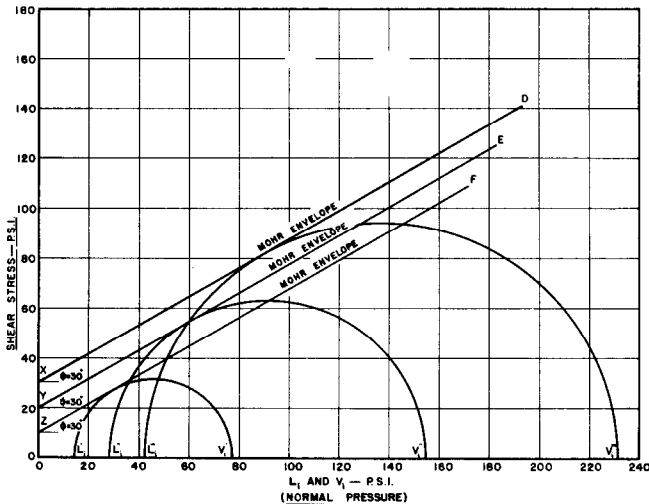


Fig. 16. Mohr Diagram Illustrating Influence of Variation of Cohesion " $c$ " on Values of  $L_1$  and  $V_1$  When Angle of Internal Friction " $\phi$ " is Constant.

for any specified magnitude of  $L_1$ , the value of  $(V_1 - L_1)$  provides a measure of the stability of a material with combined granular and cohesive properties, (fig. 21).

Fig. 17 and 18 are graphs of different values of  $L_1$  and  $(V_1 - L_1)$  respectively, in terms of  $c$  and  $\phi$ .

Fig. 19 is a stability diagram for hot mix asphaltic concrete paving mixtures, based upon the triaxial compression test, which appears in the Asphalt Institute's recent manual<sup>6</sup>. It will be observed that a single boundary appears between mixtures having combinations of  $c$  and  $\phi$  labelled satisfactory and unsatisfactory. Obviously, however, an asphalt mixture of greater stability is required in the vicinity of bus stops and traffic lights, than for average

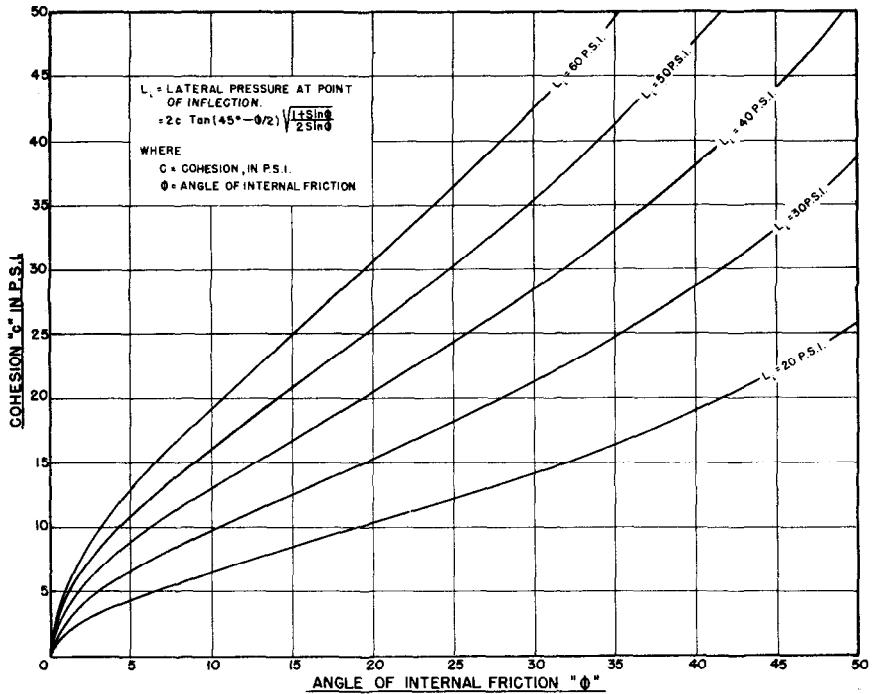


Fig. 17. Relationships between Cohesion "c", Angle of Internal Friction "φ", and Lateral Pressure at the Point of Inflection "L<sub>1</sub>" for Triaxial Compression Test

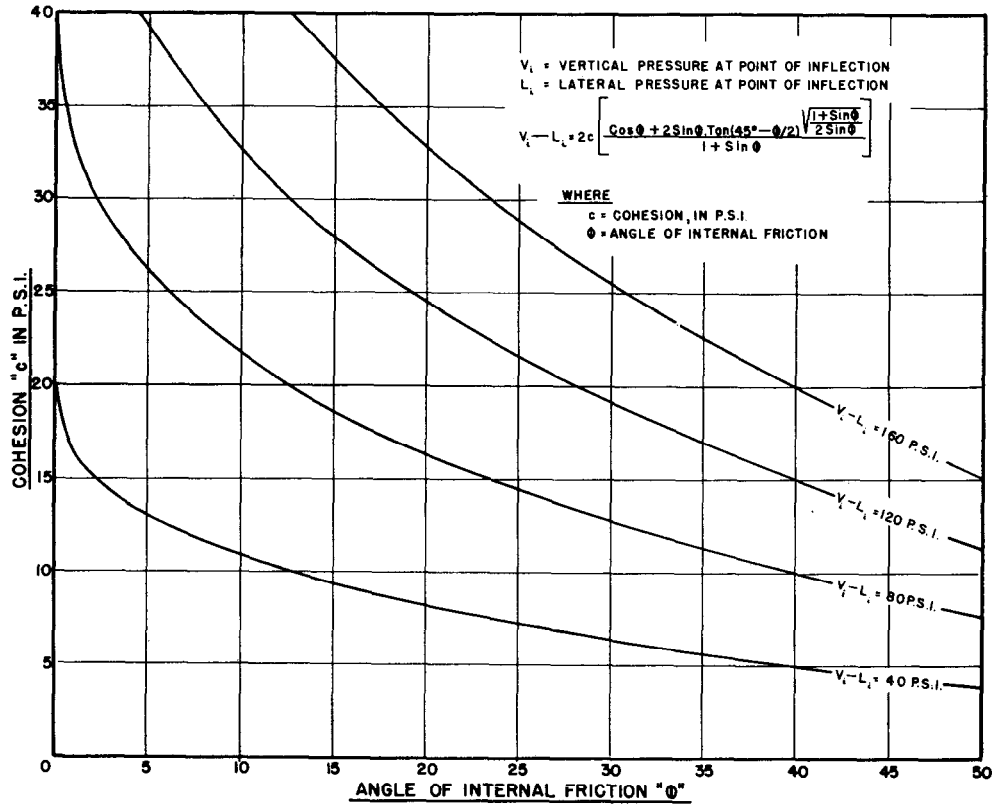


Fig. 18. Relationships between Cohesion 'c', Angle of Internal Friction "φ", and  $V_1 - L_1$  for Triaxial Compression Test.

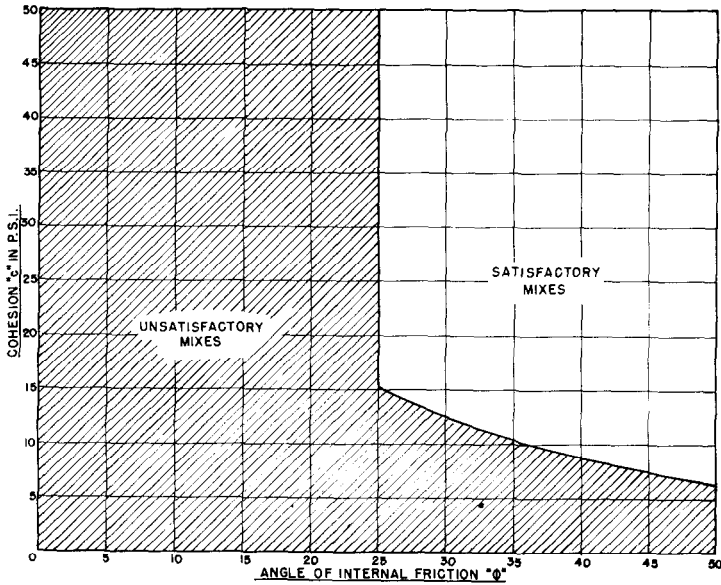


Fig. 19. Design Chart for Asphaltic Concrete Based upon the Triaxial Compression Test (The Asphalt Institute Manual on Hot-Mix Asphaltic Concrete Paving)

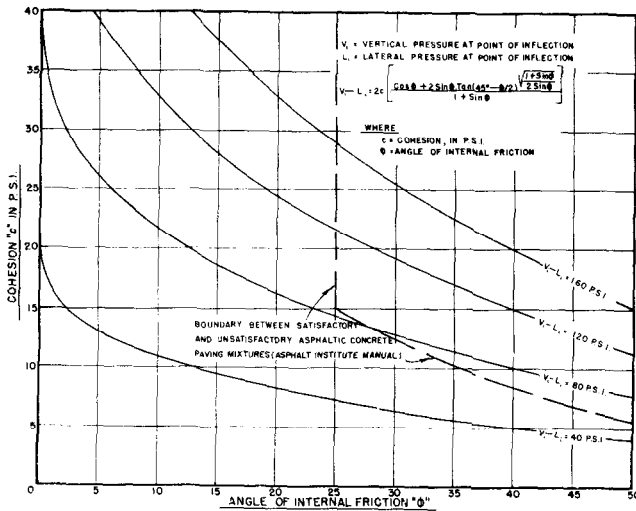


Fig. 20. Graph Showing the Boundaries between Satisfactory and Unsatisfactory Asphaltic Concrete Mixtures Proposed by the Asphalt Institute, and  $V_1 - L_1$  Values.

traffic conditions. The diagram of fig. 19 does not indicate the combinations of  $c$  and  $\phi$  required for increased or decreased pavement stability. It is clear therefore, that the utility of this diagram would be materially increased if it could be zoned into areas of greater or less stability.

In fig. 20 ( $V_1 - L_1$ ) curves are superimposed upon the Asphalt Institute diagram of fig. 19. It should be noted that the curve representing a ( $V_1 - L_1$ ) value of 80 p.s.i. coincides quite well with the lower boundary for satisfactory mixtures shown in the Asphalt Institute diagram, although better agreement would probably be obtained with the curve for a ( $V_1 - L_1$ ) value of 70 p.s.i. For locations such as bus stops or traffic lights, where high stability is required, bituminous mixtures might be specified that have corresponding values of  $c$  and  $\phi$  which result in a ( $V_1 - L_1$ ) value of 120 p.s.i. or higher. For average conditions, bituminous mixtures having combinations of  $c$  and  $\phi$  which result in a ( $V_1 - L_1$ ) value of 80 p.s.i., might be satisfactory. The ( $V_1 - L_1$ ) values required by bituminous pavements for different traffic conditions, could be determined by investigations in which field performance was correlated with triaxial tests on representative pavement samples.

In fig. 21, values of  $L_1$ , the lateral support at the point of inflection, from fig. 17, have been superimposed upon the ( $V_1 - L_1$ ) curves of fig. 20. These is a maximum lateral support  $L$ , which each bituminous pavement can develop in service, and the different possible values of this lateral support  $L$ , for corresponding ( $V_1 - L_1$ ) curves, are indicated by the  $L_1$  curves of fig. 21.

If a bituminous pavement must support a vertical load  $V$  of 150 p.s.i., and the maximum lateral support  $L$  which it can develop is 50 p.s.i., the required stability ( $V - L$ ) of the paving mixture is 100 p.s.i. The solution to this problem of paving mixture design is indicated graphically in fig. 22. Only those bituminous mixtures having combinations of  $c$  and  $\phi$  which are on or to the right of the line labelled ( $V - L$ ) = 100 p.s.i.,  $L$  = 50 p.s.i., and above the ( $V_1 - L_1$ ) curve labelled 100 p.s.i., would have the required stability and cohesion. Those paving mixtures with combinations of  $c$  and  $\phi$  falling within the cross-hatched area of fig. 22, would be deficient in either stability or cohesion  $c$  insofar as the particular conditions of design for this problem are concerned.

In the Asphalt Institute diagram, figs. 19 and 22, the left-hand boundary between satisfactory and unsatisfactory paving mixtures is a vertical line. Fig. 22, on the other hand, indicates that this left-hand boundary should

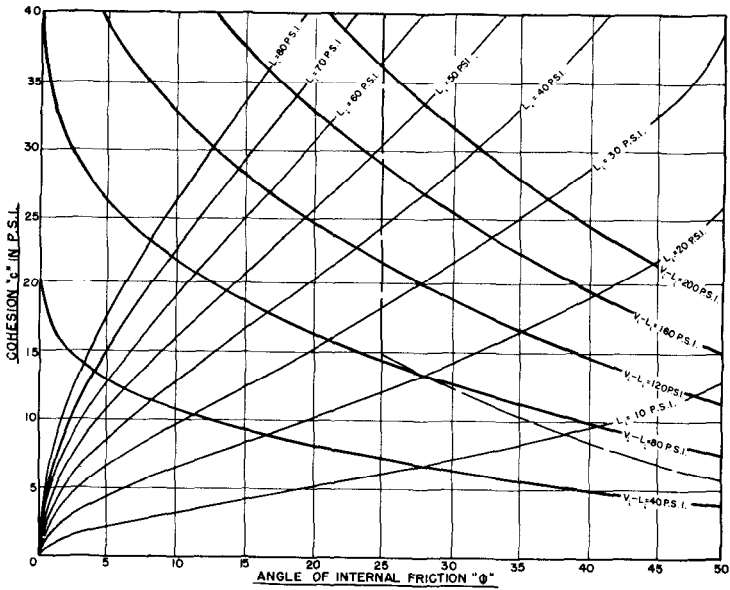


Fig. 21. Chart for Asphaltic Concrete Design Based upon Values of  $c$ ,  $\phi$ ,  $L_1$ , and  $V_1 - L_1$  Derived from the Triaxial Compression Test

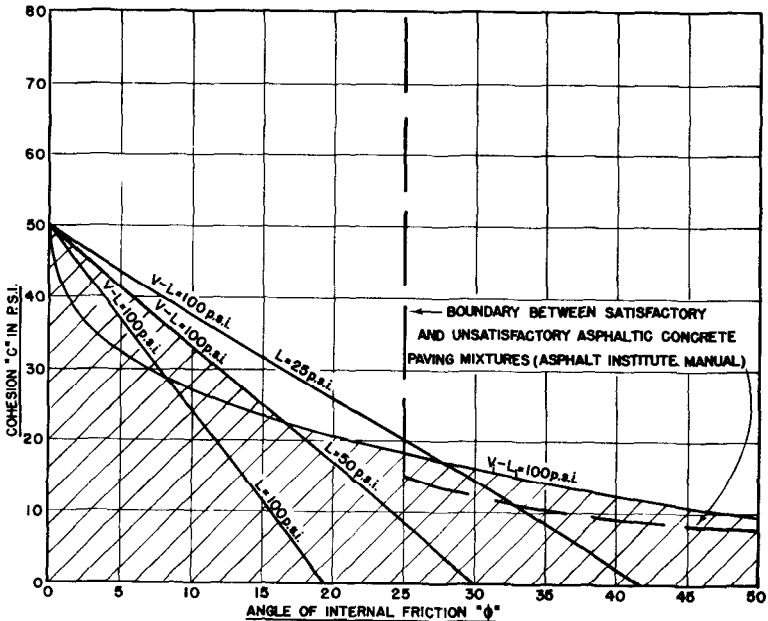


Fig. 22. Use of Stability Curves (V-L) and ( $V_1 - L_1$ ) for Flexible Surface Design

consist of portions of two curves. Its position is not vertical, but slopes far toward the left. Consequently, fig. 22 indicates that the Asphalt Institute diagram is much too restrictive, and that satisfactory stability will be obtained for bituminous mixtures with a much wider range of  $c$  and  $\phi$  values than it would permit.

This approach, based upon  $(V_1 - L_1)$  curves, provides minimum values for cohesion  $c$  for bituminous mixture design, that appear to be in reasonable agreement with the experimental information already obtained. This is illustrated in fig. 20, where it is apparent that a  $(V_1 - L_1)$  curve for 70 p.s.i. corresponds very well with the lower boundary for satisfactory mixtures on the Asphalt Institute diagram, which was prepared empirically, by correlating the  $c$  and  $\phi$  values of bituminous pavements, as measured by triaxial compression test, with their service performance in the field.

#### 6. Influence of Braking Stresses

When the brakes are applied to the wheels of a moving vehicle, a horizontal thrust is developed within the pavement. A similar effect but in the opposite direction occurs when a vehicle is accelerated. This horizontal thrust decreases the effective lateral support within the pavement which is available for supporting the vertical load on the wheel. Fig. 23 demonstrates in a quantitative manner, the influence which this horizontal thrust due to braking or accelerating stresses may have on the design of a bituminous paving mixture.

If the vertical load  $V$  to be carried is 150 p.s.i., and the maximum lateral support  $L$  available is 50 p.s.i., under ordinary traffic conditions, ( $V - L = 100$  p.s.i.) only those paving mixtures with combinations of  $c$  and  $\phi$  to the right of the area in single hatching in fig. 23, would have sufficient stability, that is, above the curve  $(V_1 - L_1) = 100$  p.s.i. and to the right of the curve  $V - L = 100$  p.s.i.,  $L = 50$  p.s.i. However, if due to braking stresses, the effective lateral support  $L$  is reduced to 25 p.s.i., then fig. 23 demonstrates that to carry a vertical load  $V$  of 150 p.s.i., ( $V - L = 125$  p.s.i.), only those bituminous mixtures with combinations of  $c$  and  $\phi$  to the right of the double hatched area, would have the required stability, that is, above the curve  $(V_1 - L_1) = 125$  p.s.i., and to the right of the curve  $V - L = 125$  p.s.i.,  $L = 25$  p.s.i.

Consequently, the double hatched area represents the increase in pavement stability that may be required because of braking or accelerating stresses (braking stresses are usually more severe). Fig. 23 makes it clear why paving

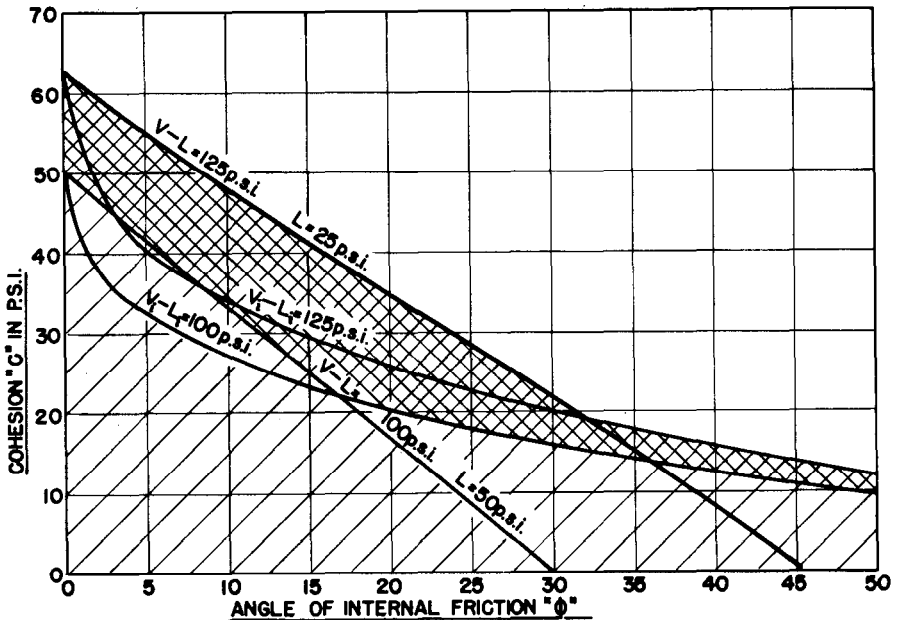
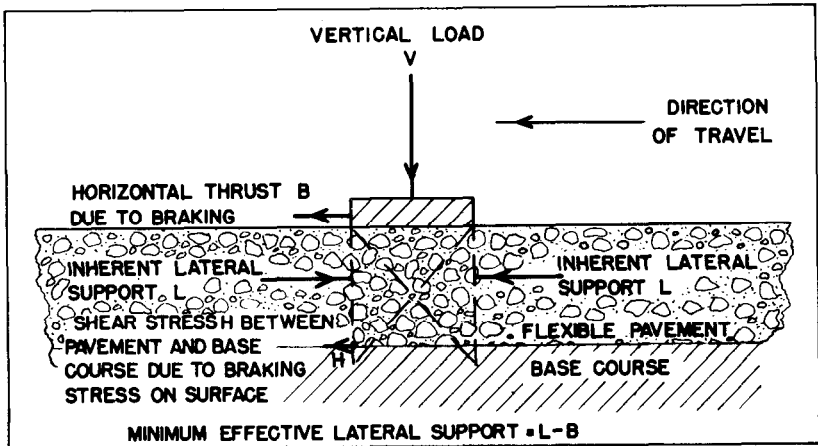


Fig. 23. Influence on the Design of Flexible Pavement Mixtures of Change in Lateral Support Due to Wheel Load Braking



mixtures with little more than sufficient stability for average locations, distort badly at stop signs and traffic lights, when there is much stopping and starting of traffic.

Fig. 23 demonstrates that the horizontal thrust  $B$  at the pavement surface due to braking, tends to create a shear stress  $H$  at the interface between the pavement and the base course. This shear stress  $H$  in turn, reduces the effective lateral support  $L$  within the underlying base course. Because of this lowering of effective lateral support, a more stable base course material is also required to support a given vertical load at all points where there is much stopping and starting of traffic. This can be illustrated by reference to the lower diagram of fig. 23. If the vertical load  $V$  to be carried by the base course is 150 p.s.i., and the maximum lateral support available under ordinary traffic conditions is 50 p.s.i., ( $V - L = 100$  p.s.i.), only those base course materials, with combinations of  $c$  and  $\phi$  to the right of the curve labelled  $V - L = 100$  p.s.i., and  $L = 50$  p.s.i., would have the required stability. However, if due to braking stresses at the pavement surface, the effective lateral support in the base course is reduced to 25 p.s.i., fig. 23 demonstrates that to carry a vertical load  $V$  of 150 p.s.i., ( $V - L = 125$  p.s.i.), only those base course materials with combinations of  $c$  and  $\phi$  to the right of the line designated  $V - L = 125$  p.s.i.,  $L = 25$  p.s.i., would have the necessary stability.

Consequently, at bus stops, traffic lights, and all other locations where there is much breaking or accelerating of traffic, not only must the bituminous pavement have greater stability to withstand the stresses of stopping and starting, but the underlying base course material must have greater stability than would otherwise be necessary. For similar reasons, this is also true of sections of pavement on slopes, particularly with steep gradients, as compared with level areas.

To make the presentation as simple as possible, the above discussion has avoided consideration of secondary vertical reactions which are caused by braking stresses. However, these could be added to the other vertical forces involved, and the same method of solution followed.

## 7. General

1. It should be particularly noted that the development based upon the triaxial compression test which has been outlined here, places the design of base courses and flexible wearing surfaces on a pounds per square inch basis.

2. It is to be observed that fig. 22 can be employed by itself to determine the minimum value of  $c$  for a purely cohesive material, the minimum value of  $\phi$  for a purely granular material, or the required combinations of  $c$  and  $\phi$  needed by materials having both cohesive and granular properties to function as either base or wearing courses. One extremity of the curve  $(V - L) = 100$  p.s.i.,  $L = 50$  p.s.i., in fig. 22, cuts the  $c$  axis at  $c = 50$  p.s.i., the minimum value of cohesion which a purely cohesive material must have for this particular problem. The other extremity of this  $(V - L)$  line cuts the  $\phi$  axis at  $\phi = 30^\circ$ , the minimum values of  $\phi$  required for a purely granular material. Only the combinations of  $c$  and  $\phi$  to the right of this  $(V - L)$  line satisfy the stability requirements of this problem for base course materials, while the curve for  $(V_1 - L_1) = 100$  p.s.i., imposes the special restrictions which are needed to provide suitable paving mixtures for the surface course. Consequently, the special stability diagrams of figs. 5 and 8, for purely cohesive and purely granular materials respectively, are unnecessary, since the same information can be derived from the general stability diagrams of figs. 10, 12 and 22, etc.

3. The amount of lateral support  $L$  which can be developed by a base course or flexible pavement for an airport or highway is largely unknown at the present time. However, by means of the development which has just been outlined, it is believed that the lateral support  $L$  for existing base courses and bituminous pavements can be evaluated by suitable investigations which would include field observations and laboratory tests. The values of  $c$  and  $\phi$  for the material being investigated can be determined by the triaxial compression test, and the maximum unit vertical load  $V$  supported by the material can be measured or calculated from vehicle tire pressure, corrected by a suitable factor for dynamic loading where necessary.<sup>7</sup> This would leave the lateral support  $L$  as the only unknown in the general stability equation (6), and its value could therefore be readily calculated. Dynamic factors associated with moving vehicles, and other variables, may make the problem more complicated, but this method for evaluating the degree of lateral support  $L$  appears to be reasonable as a first approach. It might be expected that lateral support  $L$  would vary with the thickness of the wearing course or base course layer, with the composition, density, and moisture content of the material, and with the size of the contact area of the applied load. Suitable tables for values of  $L$  might be prepared, for which these different variables were taken into account.

4. It should be emphasized that the values of  $c$  and  $\phi$  obtained for any given material depend on the procedure employed for the triaxial test. This fact has been very carefully pointed out by Endersby<sup>5</sup> and others. No standardized procedure for this test has yet been established, and several different methods are being employed. The size of sample and its dimensions, the method of preparation of the sample, the speed of testing, the size of the largest particle, absence or freedom of drainage, the temperature of test, and the procedure for applying lateral and vertical pressures, are some of the variables that must be considered. For the design of base courses and bituminous mixtures for stability, for example, the procedure devised for the triaxial test would seem to require close correlation with the conditions that exist on a roadway or runway.

Consequently, before the stability equations and diagrams based on a straight line Mohr diagram, which have been outlined above, can be employed, a satisfactory procedure for the triaxial compression test must be devised. It must provide values for  $c$  and  $\phi$  which are truly representative of conditions as they exist in the field. It should also be noted that a standardized procedure for the triaxial test must be developed before the results obtained by investigators in different laboratories can be placed on a common basis of comparison.

5. Fig. 24 illustrates how an extrusion test, or any of the ordinary compression tests, could register high stability for a sample of a bituminous paving mixture in the laboratory, which would later be found to be unstable in the field. If a bituminous pavement for a given project can develop a maximum lateral support  $L$  of 50 p.s.i., and must carry a vertical load of 150 p.s.i., only those paving mixtures with combinations of  $c$  and  $\phi$  to the right and above the cross-hatched area of diagram A would have the required stability.

An extrusion test or any one of the ordinary compression tests might register high stability for a bituminous mixture having the  $c$  and  $\phi$  values,  $c = 25$  p.s.i., and  $\phi = 9^\circ 45'$ , represented by point X in diagram A of Fig. 24. For point X, diagram A indicates a  $V - L$  value of 100 p.s.i., if a lateral support of 100 p.s.i., can be developed. That is, a vertical load  $V$  of 200 p.s.i. could be supported by a bituminous mixture represented by point X, if it could develop a lateral support of 100 p.s.i. This combination of  $V$  and  $L$  values is represented by the full line Mohr circle in diagram B of fig. 24. However, the maximum lateral support  $L$  available, is only 50 p.s.i. The broken line Mohr

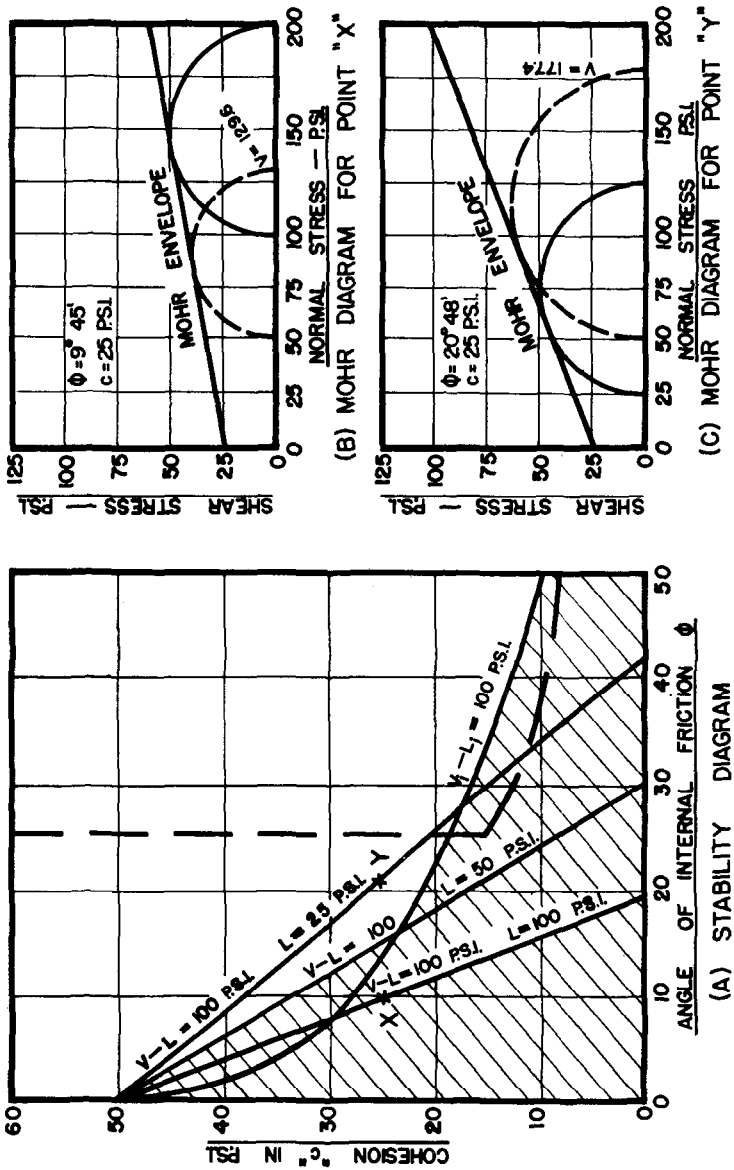


Fig. 24. Conditions of Stability and Instability in terms of "c" and "phi" which Govern the Selection of Base Course and Flexible Surfacing Materials with Respect to a Given Design Requirement

circle of diagram B of fig. 24 indicates that the bituminous mixture represented by point X could support a vertical load  $V$  of only 129.6 p.s.i., if the lateral support were 50 p.s.i. According to the conditions of the problem, it must be capable of supporting a vertical load  $V$  of 150 p.s.i. at a lateral support of 50 p.s.i. Consequently, the bituminous mixture represented by point X in diagram A of fig. 24 does not have the stability required for the conditions of this project.

In the extrusion test, the sample is rigidly confined within a steel cylinder when vertical load is applied. The amount of lateral support provided for the sample is therefore indeterminate, probably variable from mixture to mixture, and likely quite high. For any of the ordinary compression tests, the lateral support provided is zero, or essentially so. Consequently, since neither the extrusion nor the ordinary compression tests provide test conditions similar to those to which a bituminous pavement is subjected in the field, they may provide entirely erroneous measurements of the stability which a bituminous mixture will be able to develop under service conditions, as the above example has illustrated.

Section C of fig. 24, is a Mohr diagram for point Y in part A of this figure. Point Y represents corresponding  $c$  and  $\phi$  values of  $c = 25$  p.s.i., and  $\phi = 20^{\circ}48'$ . Point Y also indicates that if the lateral support  $L$  available is 25 p.s.i., the maximum vertical load  $V$  which can be carried is 125 p.s.i. This is illustrated by the full line Mohr circle in diagram C. The question might be asked that if the bituminous mixture with the  $c$  and  $\phi$  values represented by point Y in diagram A can support a vertical load of only 125 p.s.i. when the lateral support is 25 p.s.i., will it be able to carry a vertical load of 150 p.s.i., as required by this problem, when the lateral support is 50 p.s.i.? The answer is given by the broken line Mohr circle of diagram C, which shows that for a lateral support of 50 p.s.i., this bituminous mixture will be stable under a maximum vertical load of 177.4 p.s.i.

6. While stability has been considered in terms of  $(V - L)$  values in this paper, it is to be noted that each  $(V - L)$  value can be converted into shearing resistance. The maximum shearing resistance that a material can develop for corresponding values of  $V$  and  $L$  is  $(V - L)/2$ , and it occurs on planes making an angle of  $45^{\circ}$  with the direction of the principal stresses. The maximum shearing resistance on the plane of failure is given by the equation

$$s_m = \frac{V - L}{2} \cos \phi \quad (12)$$

where  $s_m$  = the maximum shearing resistance on the plane of failure, and the other symbols have the significance already attributed to them.

If required, stability diagrams can be very easily prepared in terms of  $s_m$  rather than  $(V - L)$  values.

7. It should be noted that the development presented in this paper is concerned with evaluating the stability of various materials. In the design of bituminous mixtures, other characteristics such as density, durability, etc., must always receive a great deal of attention. However, after all these other matters have been given due consideration, the development which has been outlined here makes it possible to determine whether or not the resulting paving mixture will have the stability required, and if not, in what direction its design must be modified in order that it will have adequate stability.

8. The development presented in this paper would seem to have value for solving stability problems in other divisions of soil mechanics, e.g., the selection of materials for, and the design of earth dams, embankments, foundations, etc. It should also be observed that if the maximum major principal stress  $\sigma_1$ , supported in equilibrium by an element at any given point in a structure could be measured or calculated, and the  $c$  and  $\phi$  values for the material at that point were determined in the laboratory, the maximum minor principal stress  $\sigma_{11}$  acting on the element could be calculated by means of equation (6).

### Summary

1. Equations of stability have been derived, and stability diagrams have been prepared, for purely cohesive and purely granular materials, and for materials having both cohesive and granular properties, on the basis of the geometrical and trigonometrical properties of a straight line Mohr envelope for triaxial compression data.

2. The application of these stability equations and stability diagrams to the selection of base course materials, and to the design of bituminous paving mixtures for airports and highways, etc., has been illustrated.

Acknowledgment

This paper presents the results from one phase of the comprehensive investigation of the runways at a number of Canadian airports, which has been carried on by the Dominion Department of Transport since early 1945. General administration of this investigation has been in the charge of Mr. F. C. Jewett, Chief, Wartime Construction, until his recent retirement, and of Mr. Theo. Ward, Assistant Chief, Wartime Construction. Since Mr. Jewett's retirement, general administration has been under Mr. Charles Flint, Superintendent, Construction. In their respective districts, the testing program has been carried on with the generous cooperation of District Airway Engineers E. F. Cooke, John H. Curzon, Homer P. Keith, W. C. MacDonald, George W. Smith, and A. L. H. Somerville.

In the preparation of the material upon which this paper is based, special mention should be made of the able assistance provided by C. L. Perkins in particular, and by J. P. Walsh, D. S. Johnson, P. J. Prokopy, R. Applebaum, and B. H. Newington.

References

1. Norman W. McLeod "A Canadian Investigation of Flexible Pavement Design" Proceedings, The Association of Asphalt Paving Technologists, Volume 16, (1947).
2. Miles S. Kersten, "Review of Methods of Design of Flexible Pavements" Proceedings, Highway Research Board, Volume 25, 1945.
3. W. G. Holtz, "The Use of the Maximum Principal Stress Ratio as the Failure Criterion in Evaluating Triaxial Shear Tests on Earth Materials," Proceedings, American Society for Testing Materials, Volume 47 (1947).
4. Philip C. Rutledge, "Cooperative Triaxial Shear Research Program of the Corps of Engineers," Waterways Experiment Station, Vicksburg, Mississippi, April 1947.
5. L. W. Nijboer, "The Determination of the Plastic Properties of Bitumen Aggregate Mixtures and the Influence of Variations in the Composition of the Mix," Proceedings The Association of Asphalt Paving Technologists, Volume 16, 1947.
6. Manual on Hot Mix Asphaltic Concrete Paving, The Asphalt Institute, New York, N. Y., U.S.A. (1945).

7. E. F. Kelley, "Application of the Results of Research to the Structural Design of Concrete Pavements," Public Roads, Volume 20 No. 5, July 1939.
8. V. A. Endersby, "The Mechanics of Granular and Granular-Plastic Materials With Special Reference to Bituminous Road Materials and Subsoils," Proceedings, American Society for Testing Materials, Volume 40, (1940).

Discussion

MR. V. A. ENDERSBY: One point I think ought to be clarified. In order to get a straight Mohr envelope you have to have the dimensions of your specimen and other test conditions such that you don't get boundary interferences. Is that not correct?

MR. McLEOD: I am not so sure that I follow exactly what you mean, Mr. Endersby.

MR. ENDERSBY: That is, you have to have a fairly tall specimen.

MR. McLEOD: That is correct. You have to have the proper relationship of the height of the specimen to its diameter in order to measure the  $c$  and  $\phi$  values accurately.